DOI 10.1007/s11182-023-02895-3
Russian Physics Journal, Vol. 65, No. 12, April, 2023

INFLUENCE OF THE ANNEALING TEMPERATURE ON THE GRAIN STRUCTURE OF V–4Ti–4Cr ALLOY AFTER THERMOMECHANICAL TREATMENT WITH ROLLING

I. V. Smirnov, I. A. Ditenberg, K. V. Grinyaev, A. N. Tyumentsev, Yu. P. Pinzhin, and D. A. Osipov

UDC 538.911; 669.292.5; 620.186.8

The effect of annealing temperature on the grain structure and microhardness values of the V–4Ti–4Cr *alloy after thermomechanical treatment with rolling has been investigated. The specificity of the change in the texture of the* V–4Ti–4Cr *alloy with an increase in the annealing temperature was studied by x-ray diffraction analysis. Based on the EBSD analysis data, changes in the grain structure after annealing at different temperatures were revealed. The temperature intervals for the implementation of the main processes of relaxation and recrystallization of the alloy under study were revealed. The microband (layered) structural state formed after the rolling stage is characterized by a rolling texture of the {100}<110> type which is stable up to a temperature of 700°C at which partial recovery begins with relaxation of the most defective areas. At 800°C, primary recrystallization processes are activated, which at 900°C cover the entire volume of the material. An equilibrium structural state with no rolling texture is formed after annealing at 1000°C. Secondary recrystallization processes are activated at 1300°C. With an increase in the annealing temperature from 700 to 900°C, the microhardness decreases from 2.3 to 1.75 GPa. No nonequilibrium solid solutions of interstitial atoms were found in the entire annealing temperature range.*

Keywords: vanadium alloy, thermomechanical treatment, annealing, grain structure, texture, microhardness.

INTRODUCTION

One of the effective ways to improve the mechanical properties (strength and ductility) of low-activation vanadium alloys is the use of various regimes of thermo-mechanical treatment (TMT), which provide the necessary modification of the structural-phase state [1–7]. To optimize TMT methods, it is necessary to study the specifics of temperature and deformation effects at various technological stages. In addition, it is necessary to reveal the complex influence of these factors on the features of the grain, defect, and heterophase structure of alloys.

To date, the most common variant of the deformation stage of vanadium alloys processing during TMT is rolling. At the same time, the high level of manufacturability of such alloys makes it possible to achieve large values of plastic deformation at room temperature without intermediate annealing. In this work, we study the influence of the annealing temperature after the deformation stage by rolling on the grain structure, texture features, and microhardness values of the V–4Ti–4Cr alloy.

Institute of Strength Physics and Materials Science of the Siberian Branch of the Russian Academy of Sciences, Tomsk, Russia, e-mail: smirnov_iv@ispms.ru, ditenbergia@ispms.ru, kvgrinyaev@ispms.ru, atyumentsev@ispms.ru, pinzhin@ispms.ru, osipov_da@ispms.ru. Original article submitted December 26, 2022.

MATERIALS AND METHODS

We used the vanadium alloy with the composition V–4.21Ti–4.36Cr–0.013C–0.02O–0.01N (wt.%) (hereinafter V–4Ti–4Cr) obtained at the JSC Bochvar High-Technology Research Institute for Inorganic Materials (Moscow). Initial samples were obtained using TMT-I [7], the main steps of which are presented below:

1. Eight-hour homogenizing annealings of the ingot in vacuum at a temperature of 1300°C.
2. Extrusion (pressing) through a mold after heating at temperatures of 950–1000°C.
3. Several cycles of rolling and upsetting at room temperature with intermediate vacuum annealings at T = 950–1000°C.

Vacuum ($\approx 2 \cdot 10^{-5}$ Torr) annealings for 1 hour were carried out at temperatures of 700, 800, 900, 1000, 1100, 1200, 1300, 1400, 1500, and 1600°C. Electron BackScatter Diffraction (EBSD) patterns [8] were obtained using a Thermo Fisher Apreo 2 S (20 kV) scanning electron microscope equipped with an EDAX VelocitySuper backscattered electron detection system. Orientation maps of the grain structure were obtained in the mode with hexagonal pointing. Kikuchi patterns formed by backscattered electrons were automatically indicated by the EDAX APEX EBSD software. The obtained data array was processed using the EDAX OIM analysis software. Samples for research were prepared by mechanical grinding and subsequent electrolytic polishing in a 20% sulfuric acid solution in methanol at a voltage of 15 V. X-ray analysis was performed on an X-ray diffractometer Shimadzu XRD 6000 (CuKα radiation). The analysis was carried out using the Powder Diffraction File 4 (PDF-4) database and the POWDER CELL 2.4 full profile analysis software. Microhardness (HV) was determined by Vickers diamond pyramid prints on a Neophot 21 device at a load of 0.5 N and dwell time of 15 s.

RESULTS AND DISCUSSION

Features of the heterophase structure of the V–4Ti–4Cr alloy after TMT-I with stabilizing annealing at 1000°C were discussed in detail in [7]. Figure 1 shows the grain structure orientation maps of the studied alloy after the rolling stage (Fig. 1*a*) and one-hour annealings at different temperatures (Fig. 1*b–i*).

As can be seen, immediately after rolling (Fig. 1*a*), the structure is highly anisotropic and is represented by bands stretched in the rolling direction (RD). The width of the bands in the direction perpendicular to the RD varies from tenths of a micron to several microns. In most of the bands, a gradient color is observed, indicating the presence of structural states with continuous small-angle misorientations. In addition, many wide bands are fragmented by discrete small-angle misorientation boundaries. After annealing at 700°C, the structure is almost identical to the initial one (Fig. 1*a*).

Annealing at 800°C (Fig. 1*b*) is characterized by the appearance of both individual grains, ranging in sizes from a few tenths of a micron to 10 μm, and grain clusters against the background of the band structure. The emerging grains are either almost equiaxed or elongated in the RD with the non-equiaxiality coefficient in the range from 1:2 to 1:4. An important feature is the fact that the boundaries of recrystallized grains are mainly misorientation high-angle boundaries. In the band structure, as before, the gradient color is preserved, while in the grains formed during annealing, the color is uniform.

Significant changes in the grain structure are observed after annealing at 900°C (Fig. 1*c*). The initial structural state is preserved only in the form of separate narrow (3–5 μm) bands up to 200 μm long propagating in the RD direction. The bulk of the material is presented by small (3–10 μm) and large (up to 30 μm) grains. At the same time, small grains are predominantly characterized by an almost equiaxed shape, while among large grains, many have the shape elongated in the RD with non-equiaxiality coefficient from 1:2 to 1:5. A weak gradient color is observed only in fragments of the initial structural state.

The legacy of the initial structure almost completely disappears after annealing at 1000°C (Fig. 1*d*). In general, the grain structure is homogeneous and is presented by almost equiaxed grains ranging in size from 15 to 30 μm with high-angle boundaries. Extremely rare are grains with sizes of 10 μm or less, which apparently are parts of the grains after the section preparation. The legacies of the initial state are chains of equiaxed grains propagating in the rolling direction.

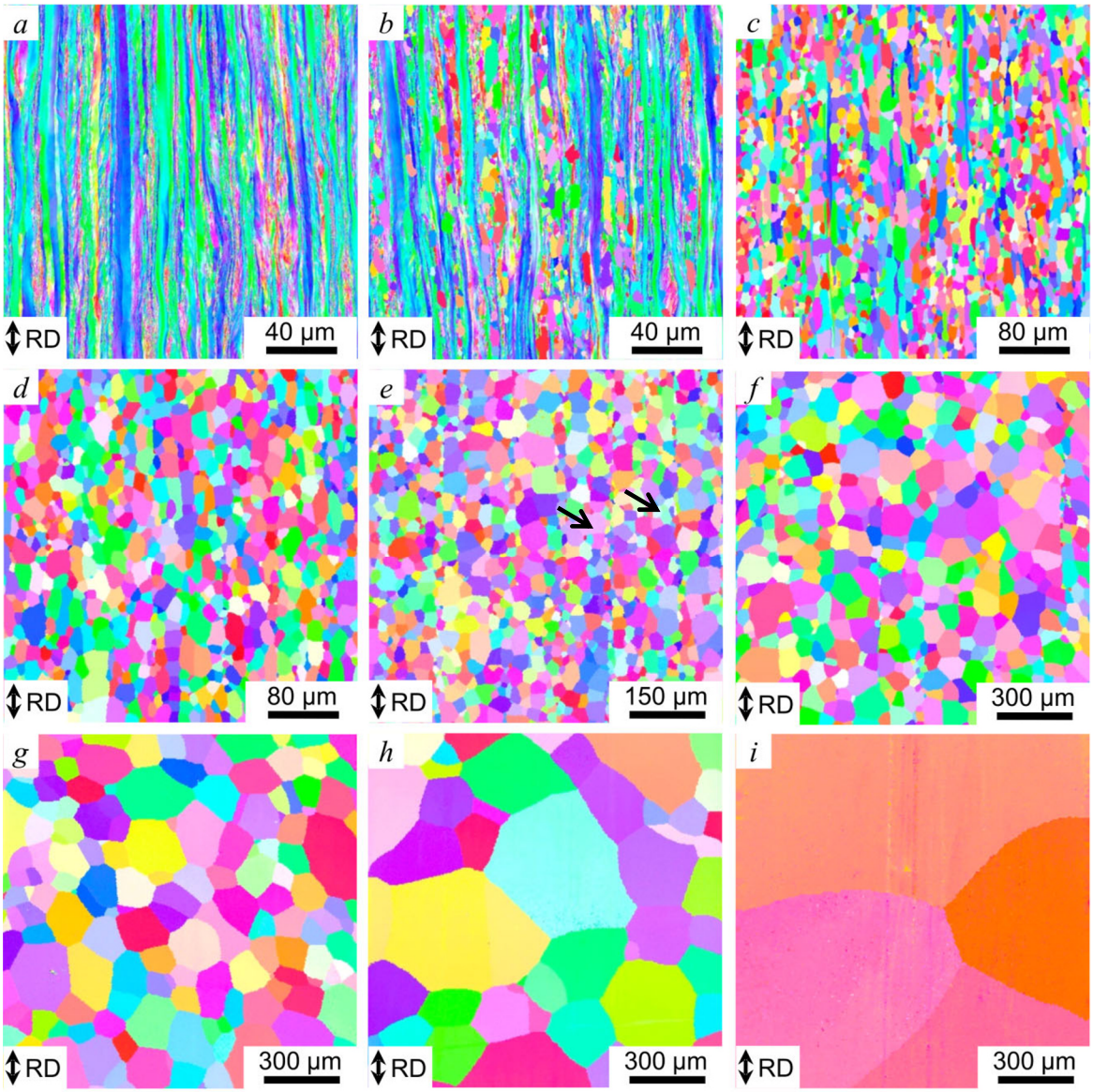

Fig. 1. Microstructure of the V–4Ti–4Cr alloy after the deformation stage of TMT (*a*) and annealings at 800 (*b*), 900 (*c*), 1000 (*d*), 1100 (*e*), 1200 (*f*), 1300 (*g*), 1400 (*h*), and 1600 °C (*i*). SEM/EBSD.

In contrast to annealing at 1000°C, the grain structure after annealing at 1100°C (Fig. 1*e*) is characterized by strong inequigranularity. In fact, two fractions of grains are clearly represented. The first fraction is formed by grains ranging in size from 10 to 20 μm. The second fraction consists of larger grains, up to 50 μm in size. The gradient color is absent in all grains. It is important to note that smaller grains decorate the position of some of the initial grain boundaries of the banded structure propagating in the RD. During annealing at 1200°C, dramatic grain growth is activated (Fig. 1*f*). In general, the structural state is homogeneous and is presented in the form of a composition of grains with a size of several tens of microns and large grains with sizes of 100–150 μm. In this case, small grains partially decorate the position of the original boundaries. After annealing at 1300°C, the grain size increases

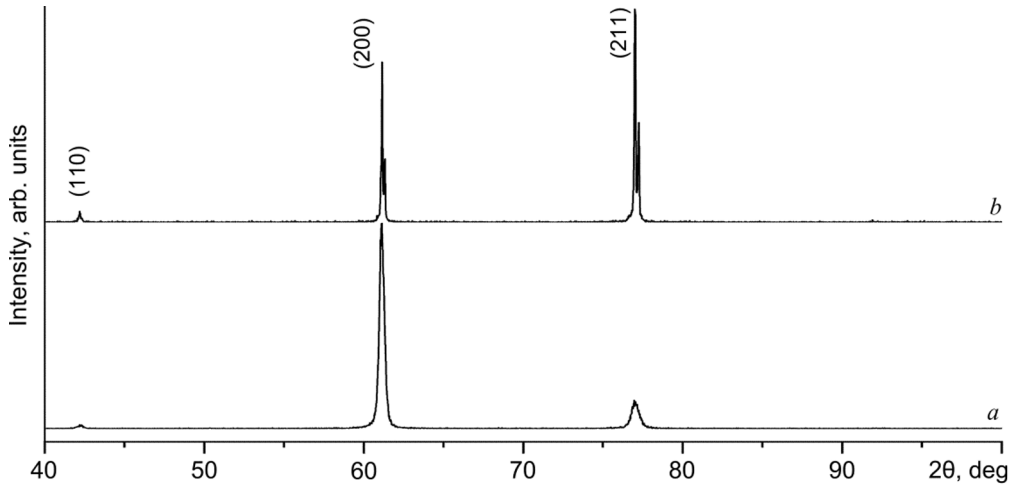

Fig. 2. XRD patterns of the V–4Ti–4Cr alloy in the initial state (*a*) and after annealing at 1000°C (*b*). X-ray was incident on the sample from the side of the rolling plane. The detector was oriented perpendicular to the RD.

approximately twofold (Fig. 1*g*) relative to annealing at 1200°C. The maximum size reaches 300 μm. The legacy of the original grain structure was not found.

A twofold increase in the grain size compared to annealing at 1300°C is observed after annealing at 1400°C (Fig. 1*h*). The maximum grain size reaches 500–600 μm. An almost identical structural state is also observed after annealing at 1500°C. At 1600°C, the grains germinate over the entire sample thickness of 1 mm (Fig. 1*i*). As is well known [8] from the EBSD analysis data, one can obtain information about the specifics of grain orientation and the presence of texture in local areas; to obtain an integral picture, it is advisable to use x-ray diffraction analysis data.

Figures 2 and 3 show examples of x-ray diffraction patterns of samples of the studied alloy in the initial state (rolling deformation stage) and after annealing at 1000°C obtained at different positions with respect to the x-ray beam. In the case of the XRD patterns shown in Fig. 2, the sample was positioned so that the x-ray beam was incident on the sample from the side of the rolling plane, with the detector oriented perpendicular to the RD. In the other case (Fig. 3), the x-ray beam is incident on the sample from the side perpendicular to the rolling plane and parallel to the RD. The detector is oriented perpendicular to the rolling direction.

It has been established that for structural states, including the initial state and annealings in the range from 700 to 900°C, on x-ray patterns, in the case of beam incidence from the side of the rolling plane (Fig. 2*a*), the absence or extremely low intensity of the diffraction peak (110) is characteristic. At the same time, it is well known [PDF entries #00-022-1058, #03-065-4776, and #03-065-6689] that for vanadium, as a BCC material, the diffraction maximum (110) is the main and characterized by 100% or unit intensity. At the same time, from the side perpendicular to the rolling plane and parallel to the RD, the peak (110) on the x-ray diffraction patterns is characterized by the maximum intensity (Fig. 3*a*). The joint analysis of x-ray diffraction patterns has made it possible to establish that after deformation by rolling, the texture is mainly represented by the {100}<110> component, which is typical for the BCC materials after this deformation method [9, 10].

After annealing at 1000°C, the x-ray patterns change significantly. In the case of beam incidence from the side of the rolling plane, the diffraction maximum (110) still has an extremely low intensity, but the maximum intensity manifests itself as a peak (211) (Fig. 2*b*). On the x-ray patterns, from the side perpendicular to the rolling plane and parallel to the RD, the peak (110) is characterized by the maximum intensity, while the intensity of the peak (211) also increases significantly. In accordance with [9, 10], such changes at high temperatures in the BCC materials can be associated with the formation and transformation of annealing textures, the study of which was not the aim of this work.

It should be noted that the x-ray diffraction analysis of the V–4Ti–4Cr alloy after TMT-I and subsequent annealings in the temperature range from 700 to 1600°C did not reveal any signs of the presence of nonequilibrium

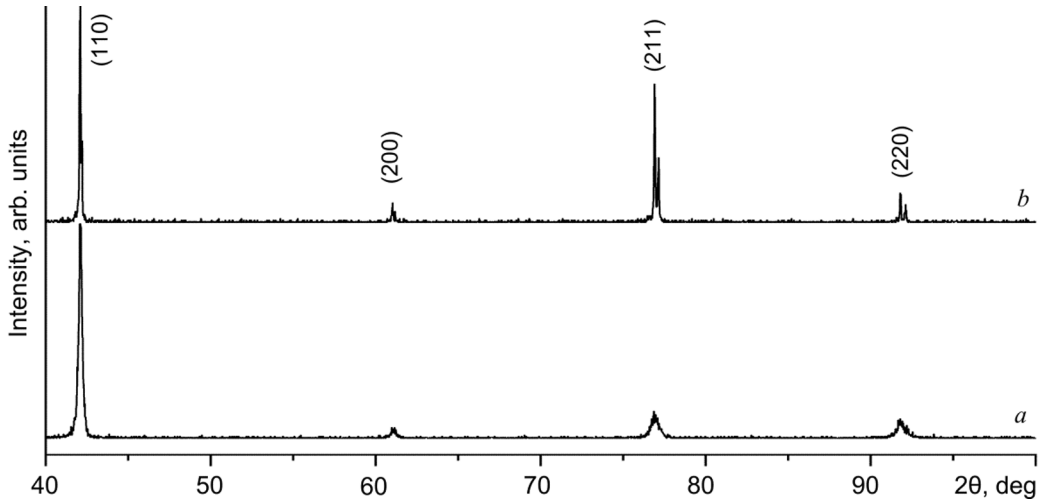

Fig. 3. XRD patterns of the V–4Ti–4Cr alloy in the initial state (*a*) and after annealing at 1000°C (*b*). X-ray was incident on the sample from the side perpendicular to the rolling plane and parallel to the RD. The detector was oriented perpendicular to the RD.

solid solutions of interstitial atoms. The above changes in the grain structure of the V–4Ti–4Cr alloy are accompanied by a decrease in the microhardness values. Immediately after the rolling cycle, the HV value reached 2.4 GPa and slightly (to 2.3 GPa) decreased after one hour annealing at 700°C. A more significant decrease in HV to 2.1 GPa was observed after annealing at 800°C. After annealing at 900°C, the microhardness values were 1.75 GPa, and during subsequent annealings remained close to this value with a small scatter (± 0.07 GPa).

In accordance with [7], at temperatures above 1300°C, partial or complete homogenization of the V–4Ti–4Cr alloy occurs, at which metastable VTi(O, C, N)-based oxycarbonitrides are intensively dissolved. In the case of TMT-I regime at annealing temperatures below the homogenization temperature, the transformation of the heterophase structure, including the formation of new stable phases, does not occur. Thus, the analyzed structural-phase states have identical phase composition.

Based on the data obtained, it is possible to distinguish the main stages of the transformation of the grain structure with an increase in the annealing temperature. The most defective initial structural state with pronounced grain anisotropy is preserved up to 700°C inclusive. In fact, this is a layered structure formed during rolling with the texture {100}<110> characteristic for the BCC materials. It is this structural state that is characterized by the highest values of microhardness. A slight decrease in the microhardness at 700°C is associated with the activation of relaxation processes, which manifest themselves in the form of a partial recovery during relaxation of the most defective states [11, 12]. In particular [12], in this alloy, after deformation by the method of torsion under pressure to values of the true logarithmic strain of 4.7–6.6, the relaxation processes of the defective submicrocrystalline (SMC) structure are activated already at 600°C.

At 800°C, the processes of primary recrystallization are already activated. Grains appearing against the background of the defective layered structure are the cause of more than 10% reduction in microhardness. In the case of annealing at 900°C, the processes of primary recrystallization cover the bulk of the material, but the elements of the microband structure and the rolling texture are retained. Such a development of primary recrystallization is the reason for a dramatic decrease in microhardness by more than 15%. For a comparison, in the defective SMC state of this alloy, more active recrystallization processes cover the entire volume of the material already at 800°C [12].

Unfortunately, for layered structures with high grain size anisotropy, the average grain size often has no physical meaning and is not a universal characteristic reflecting the specifics of the structure. Thus, the analysis of the dependence HV(d), where d is the average grain size, according to the Hall–Petch relation [13] is not possible.

Taking into account the results of [7, 11, 12], it is obvious that the thermal stability of the layered (microband) structure limited to 700 °C in the V–4Ti–4Cr alloy after TMT-I is a consequence of the insufficient volume fraction of

the second-phase fine particles. Such particles, in addition to providing effective dispersion strengthening at elevated temperatures [14, 15], are able to fix grain boundaries, which contributes to an increase in the thermal stability of the material.

After completion of primary recrystallization at 1000°C (0.58 T_{melt}), the equilibrium structural state is characterized by the absence of a rolling texture in the entire volume of the material. In the case of annealing at 1100°C, the high inequigranularity is a consequence of the high density of grain nuclei along the initial boundaries, whose growth is provoked by a dramatic thermal activation. As is well known [16, 17], one of the ways to obtain a fine-grained state is to form a high density of nuclei by various methods (deformation, spinodal decomposition, etc.) followed by annealing close to the recrystallization temperature. Simultaneous activation of the growth of a large number of grains under conditions of their competing growth leads to the formation of a fine-crystalline structural state in a certain temperature range. Such an operation can be repeated several times, up to the formation of a submicron grain size. This approach can also be implemented at temperatures below the temperature of the onset of secondary recrystallization, which is characterized by the growth of individual grains due to the absorption of the rest. Partially similar effects also appear in the case of annealing at 1200°C. Annealing at 1300°C (0.72 T_{melt}) is characterized by the onset of secondary recrystallization, which develops rapidly with a subsequent increase in temperature. In this case, the microhardness, as noted above, remains practically unchanged.

CONCLUSIONS

After the rolling stage, a microband structure is formed, which is characterized by strong grain anisotropy. In the rolling direction, the grains are elongated up to several hundred microns, while in the perpendicular direction, the grain sizes range from tenths of a micron to several microns. In addition, the layered structure obtained after rolling has a rolling texture of the {100}<110> type.

The temperature intervals for the implementation of the main relaxation and recrystallization processes of the alloy under study are revealed. At 700°C, despite the partial recovery during relaxation of the most defective states, the original structure is generally preserved. Primary recrystallization processes are activated at 800°C, and at 900°C, they already cover the entire volume of the material. After annealing at 1000°C (0.58 T_{melt}), an equilibrium structural state is formed in the entire volume of the material with no rolling texture. Annealing at 1300°C (0.72 T_{melt}) is characterized by the onset of secondary recrystallization processes. The annealing temperature increase in the range of implementation of the recovery and primary recrystallization processes (700–900°C) leads to a microhardness value decrease from 2.3 to 1.75 GPa. The formation of nonequilibrium solid solutions of interstitial atoms was not detected by the x-ray diffraction analysis over the entire temperature range of the annealings performed.

The authors are grateful to Professor V. M. Chernov and M. M. Potapenko (JSC Bochvar High-Technology Research Institute for Inorganic Materials, Moscow) for providing materials and fruitful scientific discussions. The investigation has been performed using the equipment of the Share Use Center “Nanotech” of the ISPMS SB RAS. The work was performed according to the Government Research Assignment for the ISPMS SB RAS (Project No. RW-2021-0008.

REFERENCES

1. T. Muroga, T. Nagasaka, and K. Abe, *et al.*, J. Nucl. Mater., **307**–**311,** 547 (2002).
2. N. J. Heo, T. Nagasaka, and T. Muroga, J. Nucl. Mater., **325,** 53 (2004).
3. H. Y. Fu, J. M. Chen, P. F. Zheng, *et al.*, J. Nucl. Mater., **442** (1–3)**,** S336 (2013).
4. P. F. Zheng, T. Nagasaka, T. Muroga, *et al.*, Fusion Eng. Des., **86** (9–11), 2561 (2011).
5. J. M. Chen, T. Nagasaka, T. Muroga, *et al*., J. Nucl. Mater., **374** (1–2), 289 (2008).
6. A. N. Tyumentsev, I. A. Ditenberg, K. V. Grinyaev, *et al*., J. Nucl. Mater., **413** (2), 103 (2011).
7. A. N. Tyumentsev, A. D. Korotaev, Y. P. Pinzhin, *et al*., J. Nucl. Mater., **329**, 429 (2004).

8. A. J. Schwartz, M. Kumar, and B. L. Adams, Electron Backscatter Diffraction in Materials Science, Springer, New York (2009).
9. F. J. Humphreys and M. Hatherly, Recrystallization and Related Annealing Phenomena, Elsevier, Oxford (2004).
10. D. Raabe and K. Lucke, Mater. Sci. Forum., **157**–**162**, 597 (1994).
11. I. A. Ditenberg, A. N. Tyumentsev, I. V. Smirnov, *et al*., Phys. Mesomech., **22**, 496 (2019).
12. I. A. Ditenberg and A. N.Tyumentsev, Russ. Phys. J., **60** (11), 1993 (2018).
13. E. V. Kozlov, A. N. Zhdanov, and N. A. Koneva, Phys. Mesomech., **9**, 75 (2006).
14. V. I. Trefilov, I. K. Pokhodnaya, V. F. Moiseev, and A. D. Vasiliev, Phys. Stat. Sol., **59** (2), 843 (1980).
15. B. A. Wilcox, in: Refractory Metal Alloys Metallurgy and Technology, Springer, Boston (1968), pp. 1–39.
16. F. Haessner, Recrystallization of Metallic Materials, Riederer-Verlag, Stuttgart (1978).
17. J. R. Kennedy, A. E. Davis, A. E. Caballero, *et al.*, Addit. Manuf., **40**, 101928 (2021).